Inter*net* Electronic Journal of

Molecular Design

Editor: Ovidiu Ivanciuc

Special issue dedicated to Professor Danail Bonchev on the occasion of the 65th birthday

Evaluation of 4–Azaindolo[2,1–*b*]quinazoline–6,12–diones' Interaction with Hemin and Hemozoin: A Spectroscopic, X–ray Crystallographic and Molecular Modeling Study

Rickey P. Hicks,[1] Daniel A. Nichols,[1] Charles A. DiTusa,[1] David J. Sullivan,[2] Mark G. Hartell,[1] Brandon W. Koser,[1] and Apurba K. Bhattacharjee [1]

[1] Department of Medicinal Chemistry, Division of Experimental Therapeutics, Walter Reed Army Institute of Research, Washington, DC, 20708–5100, USA
[2] Department of Molecular Microbiology and Immunology, Johns Hopkins University, Baltimore, MD, 21287, USA

Citation of the article:
R. P. Hicks, D. A. Nichols, C. A. DiTusa, D. J. Sullivan, M. G. Hartell, B. W. Koser, and A. K. Bhattacharjee, Evaluation of 4–Azaindolo[2,1–*b*]quinazoline–6,12–diones' Interaction with Hemin and Hemozoin: A Spectroscopic, X–ray Crystallographic and Molecular Modeling Study, *Internet Electron. J. Mol. Des.* **2005**, *4*, 751–764, http://www.biochempress.com.

Evaluation of 4–Azaindolo[2,1–*b*]quinazoline–6,12–diones' Interaction with Hemin and Hemozoin: A Spectroscopic, X–ray Crystallographic and Molecular Modeling Study [#]

Rickey P. Hicks,[1,]* Daniel A. Nichols,[1] Charles A. DiTusa,[1,]* David J. Sullivan,[2]
Mark G. Hartell,[1] Brandon W. Koser,[1] and Apurba K. Bhattacharjee [1,]*

[1] Department of Medicinal Chemistry, Division of Experimental Therapeutics, Walter Reed Army Institute of Research, Washington, DC, 20708–5100, USA
[2] Department of Molecular Microbiology and Immunology, Johns Hopkins University, Baltimore, MD, 21287, USA

Abstract
The 4–azaindolo[2,1–*b*]quinazoline–6,12–dione class of compounds (tryptanthrins) exhibited very strong *in vitro* activity against *Plasmodium falciparum*, as well as low cytotoxicity. Due to the structural similarity of the 4–azaindolo[2,1–*b*]quinazoline–6,12–diones with another potent antimalarial compound, chloroquine, which is known to interact with heme, the potential interactions between these compounds and heme were investigated. A series of six substituted 4–azaindolo[2,1–*b*]quinazoline–6,12–dione analogs at the 8 or 9–position were synthesized and their hemin binding affinity was determined by ¹H NMR methods. The X–ray crystal structure of a representative analogue exhibits intermolecular interactions that suggests the possibility of a heme–tryptanthrin stacking organization. This observation is consistent for proposed interactions with hemin. *Ab initio* quantum chemical calculations at the RHF/6 31G** level were conducted to aid in the understanding of the binding process. The ability of these compounds to inhibit haematin crystallization was determined using IR methods. While all investigated analogs bind via a non–covalent interaction to hemin, only the 8–nitro analog inhibited haematin crystallization.

Keywords. Malaria; tryptanthrins; NMR; X–ray crystallography; molecular modeling; *ab initio* QM calculations.

1 INTRODUCTION

The malaria parasite annually infects 300 to 500 million people worldwide, resulting in 0.5 to 2.5 million deaths each year [1]. It has been estimated that over 40% of the world's population is at risk for the disease. The most lethal of the four species of *Plasmodium* that infect humans is *Plasmodium falciparum*. Chloroquine [1] (Scheme 1) was the drug of choice for the treatment and prophylaxis of *P. falciparum* since the 1950s. Unfortunately, chloroquine resistant strains of *P. falciparum* have evolved in most locations around the world [2]. To overcome the challenges of chloroquine and other drug resistant strains of *Plasmodium*, new therapeutic agents that kill the parasite via novel mechanisms must be developed [2].

The azaindolo quinazoline–6,12–dione class of compounds [3] (Table 1) have exhibited exceptional *in vitro* activity against several drug resistant strains of *P. falciparum*, including chloroquine resistant strains, with very low cytotoxicity [2]. This class of compounds exhibits some structural similarity to chloroquine (similar to the A and B rings of the tryptanthrins). Quinoline–containing drugs accumulate in intracellular acid vesicles due to their weak base–like properties [4].
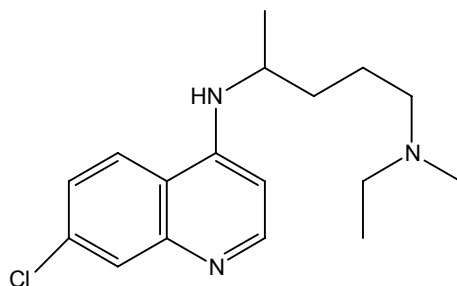
Scheme1. Structure of Chloroquine.

Many members of this family, including chloroquine, quinine and amodiaquin have significant antimalarial activity, although their specific toxicity remains unclear. It is suggested that these drugs probably inhibit a crucial metabolic step specific to the parasite at this stage in its life cycle. The antimalarial activity of chloroquine is believed to be derived from its ability to inhibit haematin polymerization [5]. This process damages membranes and inactivates haemoglobin degradation enzymes leading to parasite death [6]. In this paper we test this hypothesis and compare the ability of several derivatives of azaindolo[2,1–b]quinazoline–6,12–diones to inhibit hemin polymerization by using a combination of theoretical and experimental methods. The methods used include NMR spectroscopy, *ab initio* quantum chemical calculations, and X–ray crystallographic methods to characterize the hemin–complex.

Table 1. The four rings are labeled from left to right: A to D rings are indicated in the structure. Using the procedure described elsewhere, the IC_{50} values for the six analogs were determined against both CDC Sierra Leone (D–6, mefloquine resistant) and CDC Indochina III (W–2, chloroquine, quinine, pyrimethamine and sulfadoxine– resistant) strains of *P falciparium* [7,8].
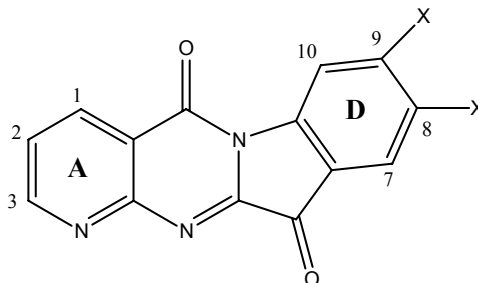
Compound number	Substituents	D6	W2
1	8–NO$_2$, 9–H	1.08	12.1
2	8–H, 9–Cl	278	263
3	8–OCF$_3$ 9–H	48	48
4	8–F, 9–H	1.54	0.84
5	8–OCH$_3$, 9–H	2.21	1.54
6	8–H, 9–H	2.36	14.6

2 MATERIALS AND METHODS

2.1 Chemical Synthesis

The azaindolo[2,1–*b*]quinazoline–6,12–dione compounds were synthesized from the condensation reaction of 3–azaisatoic anhydride (Starks) with the corresponding isatin using the method of Bergman [9]. A few of the indolo[2,1–b]quinazoline–6,12–dione (**6**, tryptanthrin) and its derivatives were obtained from PathoGenesis Corporation, Seattle, WA, USA (now owned by Chiron, Emeryville, CA). In general, these compounds can be synthesized by base–catalyzed condensation of substituted isatins and substituted isatoic anhydrides through a convenient one–step flexible synthesis as previously reported [10]. The remaining compounds mentioned herein were obtained from the in–house Chemical Information System repository [11].

2.2 NMR Methodology

Samples were prepared for the NMR studies using azaindolo[2,1–*b*]quinazoline–6,12–diones in 500 µL of DMSO–d$_6$. To these samples 100 or 200 µL aliquots of a known concentration of hemin dissolved in 1.0 mL of DMSO–d$_6$ was added. DMSO–d$_6$ was used as the solvent for these investigations instead of the traditional ethanol/water mixture due to the very poor solubility characteristic of the azaindolo[2,1–*b*]quinazoline–6,12–diones.

2.3 Quantum Chemical Computations

Calculations were performed using the *ab initio* restricted Hartree–Fock (RHF/6–31G**) calculations of quantum chemical theory as implemented in the Gaussian 94 package [12] on the binding of a sodium cation to the *pi*–face of the aromatic "D" ring of the azaindolo[2,1–*b*]quinazoline–6,12–dione analogues (Table 1). Sodium ion was chosen as the probe cation as hemin (implicitly Fe^{+2}) could not be evaluated at this level of theory. Complete geometric optimization for each complex was carried out using the above basis set. Similar calculations were performed using the geometry of the uncomplexed azaindolo[2,1–*b*]quinazoline–6,12–diones and sodium ion separately, as described in similar earlier studies [13]. The RHF/6–31G** basis set has been documented as adequate for such studies and substantially higher basis sets produce similar trends [14]. Electrostatic potential profiles at different contours of energy levels on the optimized geometry of the structures were generated to provide profiles beyond the van der Waals surface (approximately 1.4– 1.5 Å away) encountered by an approaching molecule.

2.4 Docking Calculations

We have used Docking/affinity/simulated annealing (SA) procedure of InsightII [15] for the hemin–azaindolo[2,1–*b*]quinazoline–6,12–dione interaction calculations. The Docking module allows the nonbonded energy to be calculated between two molecules using explicit van der Waals energy, explicit electrostatic (Coulombic) energy, or both van der Waals and electrostatic energies. The number of atoms included in the calculation can be limited by specifying a monomer– or residue–based cutoff. Alternatively, the computation can be done approximately using a pre–computed energy grid.

2.5 Heme Crystallization Inhibition

1 nM of both purified *P. falciparum* hemozoin and synthetic beta–hemin was incubated with 10 nM of heme substrate in 100 mM sodium acetate pH 4.8 in 200 μL of a 96–well plate for 20 hrs in a humidified 37 °C incubator [16]. A 20 mL solution with 50 μM heme and 5 nM (heme content) of heme crystal per mL was made to distribute in 200 μL aliquots in quadruplicate with serial drug dilutions of 1.25, 2.5, 5.0, 7.5, 10, and 20 μM. At the end of incubation, 50 μL of 800 mM sodium bicarbonate/1% SDS was added to dissolve unincorporated heme. The OD at 405 nm $\pm$ 15 nm measuring unincorporated heme content was recorded on a plate reader. The equation (2.1–O.D. 405nm) defines nM of new heme crystal synthesis. The error is standard deviation of four wells. The error of the line intercept with half of heme crystal growth is less than 1 nmol. Inhibition Concentrations 50% (IC_{50}) were found for the 4–azaindolo[2,1–*b*]quinazoline–6,12–dione analogs.

The nitro analog **1** yielded an IC_{50} of 4 μM for both haemozoin and beta hemin. The study did not find inhibition of heme for the other three analogs up to the 20 μM level.

2.6 X–Ray Crystal Structure Determination

The X–ray sample was a pale yellow plate (0.46 × 0.26 × 0.05 mm) crystallized from methanol. Data collection was performed at room temperature (293±2 K) on a Bruker P4 diffractometer using Cu Kα radiation and a graphite monochrometer in the incident beam. Reflections used to refine the unit cell parameters by least squares methods are as follows: 33 reflections in the range of $14° \leq 2\theta \leq 57°$. Crystal data: $C_{14}H_6FN_3O_2$, FW = 267.22, Monoclinic, P2(1)/c, a = 9.9460(10) Å, b = 8.5870(10) Å, c = 13.1120(10) Å, β= 101.000(10)°, V = 1099.3(2) Å^3, Z = 4. The data were collected using the ω scan technique with a variable scan rate ranging from 3°/min minimum to 60°/min maximum depending upon the intensity of the reflection. Three reflections were checked as intensity controls every 100 reflections and remained constant within 2.2%. No absorption correction was applied. The structures were solved using direct methods [17]. Full matrix least–squares refinement [18] was performed on coordinates and anisotropic thermal parameters for the nonhydrogen atoms, isotropic thermal parameters for the hydrogen atoms using reflections for which $|F_O| > 4\sigma(F_O)$. The hydrogen atoms were placed in idealized positions, and during refinement, the coordinates of the hydrogen atoms rode with the coordinates of the carbon to which they are attached. Final bond distances and angles were all within expected and acceptable limits.
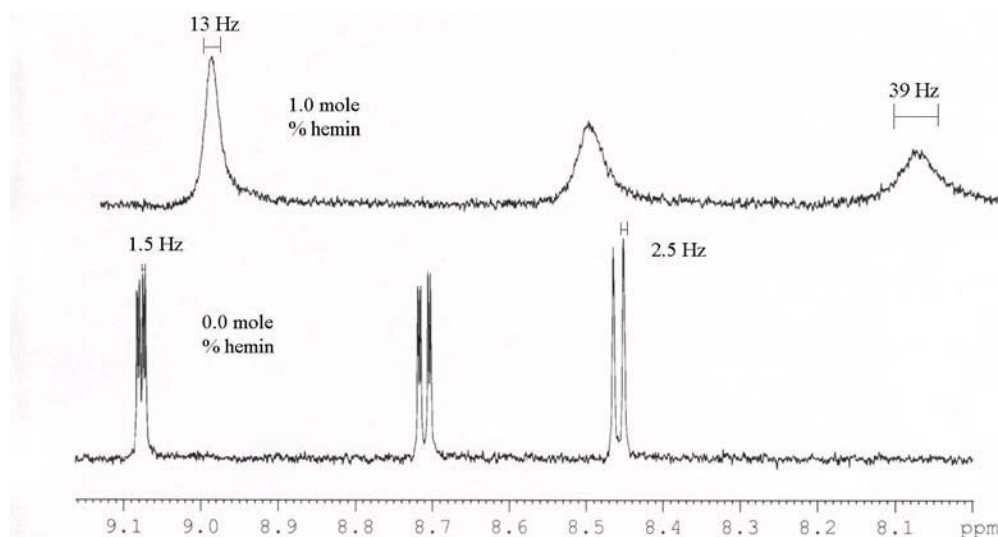

Figure 1. Bottom spectrum is of 4–azaindolo[2,1–*b*]quinazoline–6,12–dione **6** in the absence of hemin while the top spectrum is the same sample of compound **6** with 1.0 mole equivalent of hemin. These two spectra illustrate both the difference in magnitude of the chemical shift changes induced by the pseudocontact effect and the differential line broadening caused by the pseudocontact effect. The proton at approximately 9.05 ppm is shifted up field to approximately 9.01 ppm, while the proton at approximately 8.45 ppm is shifted up field to approximately 8.02 ppm; thus, in the bound form these protons are much closer to the Fe^{+3} atom. Proximity to the Fe^{+3} atom is also confirmed by increased line widths.

3 RESULTS AND DISCUSSION

3.1 NMR Analysis

The hemin binding affinity for a series of six 4–azaindolo[2,1–*b*]quinazoline–6,12–diones with functional groups having different electron donating/withdrawing characteristics was determined via ^{1}H NMR studies. The binding interaction was measured as a function of increasing hemin concentration. [1]H spectra of each analog with an increasing concentration of hemin were collected and analyzed for the effect of the pseudocontact shifts. Bio–molecules containing the paramagnetic species Fe^{+3} are known to induce up–field chemical shifts of the ^{1}H, ^{13}C, and ^{15}N atoms of bound ligands [19–21]. This induced chemical shift change is termed the pseudocontact shift. Unlike the NOE effect, the distance dependence of pseudocontact shifts is r^{-3} and is therefore effective at greater distances [21,22]. Therefore, the closer a particular proton on the ligand is to the Fe^{+3} atom, the greater the induced chemical shift. An example of the ^{1}H spectra obtained for compound **6** from this investigation is shown in Figure 1. In addition to the induced up–field shifts, protons close to the Fe^{+3} atom will experience a greater line–broadening than those protons which are further away and experience a much smaller $\Delta\delta$. The effect of the distance from the Fe^{+3} atom to the chemical shifts of the various protons on the 4–azaindolo[2,1–b]quinazoline–6,12–dione skeleton is shown in Figure 2. Clearly, the various protons experience different psedocontact shifts. These differences can be used to determine the relative orientation and distance between each proton and the Fe^{+3} atom.
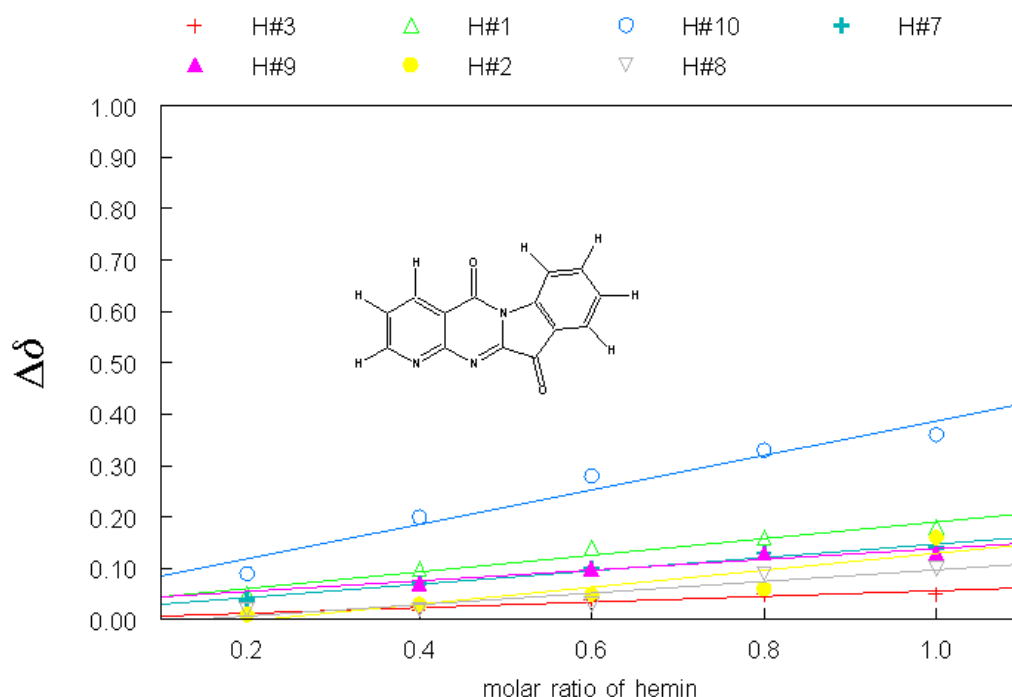

Figure 2. Plot of the pseudocontact shift for the seven protons of compound 6 as a function of increasing hemin concentration. From this plot it is clear that the following protons H10, H9 and H1 are most affected by the Fe^{+3} atom and thus are closer to the Fe^{+3} atom than are protons H2, H3, H4 and H7.

Table 2. Hemin Induced Pseudocontact Chemical Shifts

Compound	Maximum induced $\Delta\delta$ (ppm)	Slope of induced $\Delta\delta$ (ppm/mole %)
1	1.538	0.41595
2	0.389	0.11897
3	0.462	0.08951
4	0.360	0.13656
5	0.208	0.11897
6	0.558	0.09778
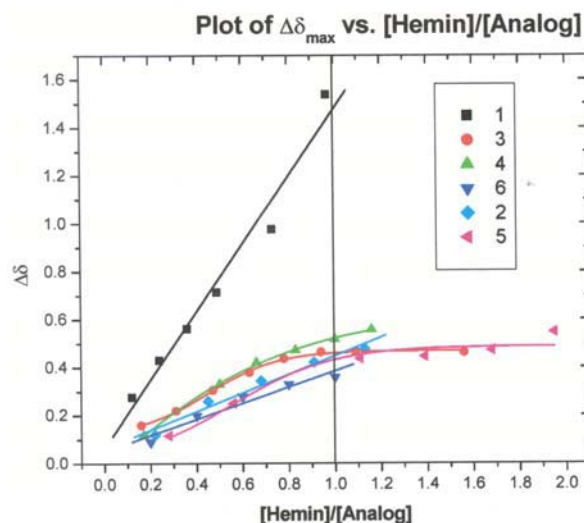
Figure 3. Plot of the maximum proton $\Delta\delta$ vs hemin concentration.
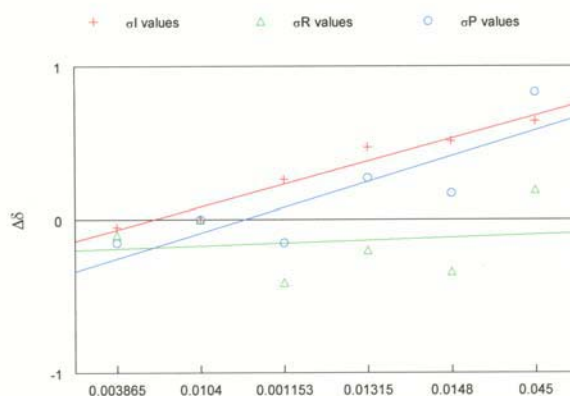
σ_I = inductive effects (red cross)
σ_P = resonance effects (green circles)
σ_Π = both resonance and inductive effects (blue circles)

|	σ_I	σ_P	σ_Π
a0	-0.214	-0.207333	-0.421333
a1	0.148286	0.018286	0.166571
Rvak	0.977706	0.154061	0.845711

Figure 4. Correlation of the electronic effects of the various substitutents with the slope of the maximum proton chemical shift induced by increasing hemin concentration.

The maximum observed pseudocontact shift ($\Delta\delta$ and the concentration dependence of this shift (slope of the plot of $\Delta\delta$ versus hemin mole%, Figure 3) for the six analogs is given in Table 2. Plotting the concentration dependence of each analog versus the σ^* (Figure 4), electron donating and withdrawing characteristics of the six substituents, indicates a clear relationship of the inductive electron donating/withdrawing character of these functional groups with hemin binding affinity.

3.2 Molecular Modeling

In order to provide a theoretical model for the NMR observations, we calculated the cation binding affinities of the D ring of the 4–azaindolo[2,1–*b*]quinazoline–6,12–dione analogues (Table 3) using a sodium ion as the cationic probe. *Ab initio* quantum chemical method was used at the restricted RHF level with 6–31G** doubly polarized basis set for complete optimization of geometry of the sodium–azaindolo[2,1–*b*]quinazoline–6,12–dione complexes and the uncomplexed azaindolo[2,1–*b*]quinazoline–6,12–dione molecules. The RHF/6–31G** calculated relative binding energies (BEs) and atomic charges of a few selected atoms in the D ring of azaindolo[2,1–*b*]quinazoline–6,12–dione analogues are presented in Table 3. Inspection of the table clearly indicates that the nitro–substituted analog **1** has a stronger cation binding affinity with the D ring than the rest of the compounds, about 16 kcal/mol more strongly than the next in the rank, the fluoro–substituted analog **4**. Compound **4** binds to sodium ion 2.3 kcal/mol more strongly than the unsubstituted analog **6** and 1.4 kcal/mol more strongly than the electron donating methoxy–substituted analog **5**. The NMR experiments on the hemin binding affinities of the compounds as depicted in their hemin induced pseudocontact chemical shifts (Table 3) indicate a clear consistency with the theoretical sodium binding affinities. In addition, the NMR experiments indicate stronger interaction of hemin with the protons associated with the D ring, particularly H10 and H9.

Table 3. Calculated total atomic charges at the different atomic centers and relative binding energy of the complexes at 6–31G** level of *ab initio* quantum chemical theory along with hemin binding affinity and Fe—H distance of the docked structures.
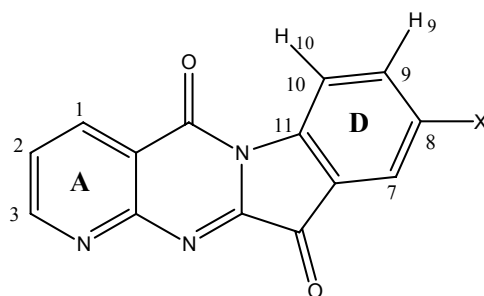
Cmpd	–X	Total Atomic Charges					Relative BE (kcal/mol)	Hemin Binding Affinity	Distance Fe..H in min energy docked structures (Å)	
		C11	C10	C9	H1	H2			H1	H2
1	–NO₂	0.42	–0.21	–0.15	0.3	0.29	35.5	0.045	5.2	4.1
4	–F	0.38	–0.18	–0.26	0.29	0.24	18.8	0.015	7.4	9.0
6	–H	0.39	–0.2	–0.18	0.28	0.22	16.5	0.010	6.9	8.6
5	–OCH₃	0.37	–0.18	–0.23	0.28	0.23	17.4	0.012	9.4	12.3

Interestingly, the calculated atomic charges on these protons as well as the three associated carbon atoms in the nitro–substituted analog **1** differ significantly from the others. The location of the cation (sodium ion) in the optimized geometry of the sodium–azaindolo[2,1–*b*]quinazoline–6,12–dione complexes of both nitro **1** and fluoro **4** analogues is found to be by the C10/C11 atom in the D ring corroborating the NMR evidence of stronger hemin interaction at these positions. The position of cation (sodium ion) in the optimized geometry of the other two complexes is found by the center of the D ring. The molecular electrostatic potential (MEP) profiles of the uncomplexed azaindolo[2,1–*b*]quinazoline–6,12–dione at −1.0 kcal/mol (Figure 5) seem to guide the site of interaction with the cation. Inspection of the figure indicates that the *pi*– electrons of the D ring in nitro compound **1** become more localized by the C11 atom due to the strong electron withdrawing effect of the substituent, and thus the cation is likely to prefer a binding site around this location. The trend is also noticeable in the electron withdrawing fluoro compound **4** though not as strongly as nitro analog **1**. The *pi*–electrons of the D ring in the unsubstituted compound **6** remain unaffected as seen from the large electron distribution over this ring (Figure 5) and thus the cation (sodium ion) in its optimized complexed structure remains over the centroid of the ring. In the methoxy compound **5**, due to the electron donating nature of the substituent, the D ring gets reinforced with electrons, which is clearly noticeable from the large electron distribution (Figure 5). This may be the reason why the binding energy with the cation (sodium ion) increases by 1.1 kcal/mol for the unsubstituted analogue, **6**.
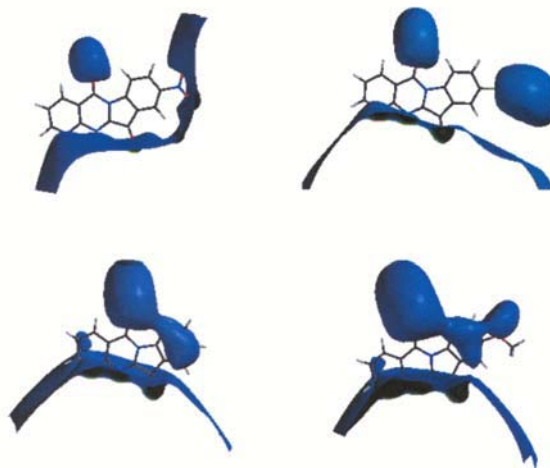

Figure 5. Electrostatic potential profiles for the selected compounds: top left **1**, top right **4**, bottom left **6**, bottom right **5** at −1.0 kcal/mol (approximately 1.3 to 1.4 Å away from the molecular surface).

In order to further understand the interaction, the complete structures of both hemin and azaindolo[2,1–*b*]quinazoline–6,12–dione analogues were considered and docking calculations using the Docking/affinity module in InsightII were performed. The force field that best describes this interaction process was found to be "esff" (electrostatic force field) as implemented in the software.

Accordingly, the potentials of both hemin and each individual azaindolo[2,1–*b*]quinazoline–6,12–dione analogue were fixed at the force field before carrying out the docking calculations. Since the distances between the Fe^{2+} ion and the two protons in the D ring were found to be the most affected in the NMR experiments we have presented the calculated nonbonded distance between Fe^{2+} and these two protons in Table 3. The data clearly indicate a stronger interaction between hemin and the nitro analog **1** than the other analogues (Table 3). Thus, this observation is also consistent with the NMR experiments as well as the model observed using the sodium ion.

3.3 X–ray Crystallographic Study

The X–ray crystal structure of representative analog 8–fluoroindolo[2,1–*b*]4–azaquinazoline–6,12–dione, **4**, (Figure 6) is found to be almost perfectly planar, with an RMS deviation of 0.0461(8) Å. This planarity, particularly through N6, suggests extended conjugation throughout much of the fused ring structure.
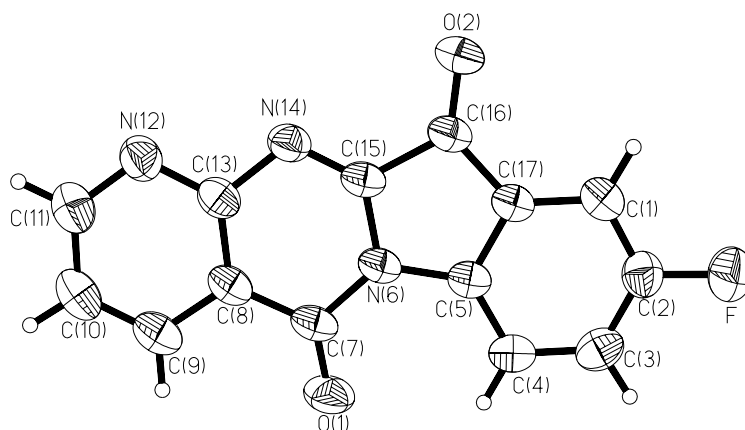

Figure 6. Thermal ellipsoid plot of molecule **4** showing the atom numbering used for the X–ray crystallographic report. Ellipsoids are drawn at the 50% probability level and H atoms are represented by circles of arbitrary radii.

The crystal packing lattice of **4** consists of a stacking column along the [001] direction without apparent π–π interactions (Figures 7 and 8). This finding is consistent with the observation that the yellow color of **4** is much less intense than that of analogs exhibiting π–stacking. In fact, alternating molecules form a crossed pattern with no A or D aromatic ring overlap between (x, y, z) and (x, y, z+1).

Although the only crystal structure presented here is that of molecule **4**, the extended conjugation of the *pi*–electrons within tryptanthrins has been observed in this laboratory [23] and elsewhere [24,25], and is likely to present in all planar analogs. Thus, the X–ray crystallographic structure of **4** clearly demonstrates the possibility of stacking interactions in these molecules in conformity with our NMR and molecular modeling observations of a probable *pi*–type weak interaction with the hemin.
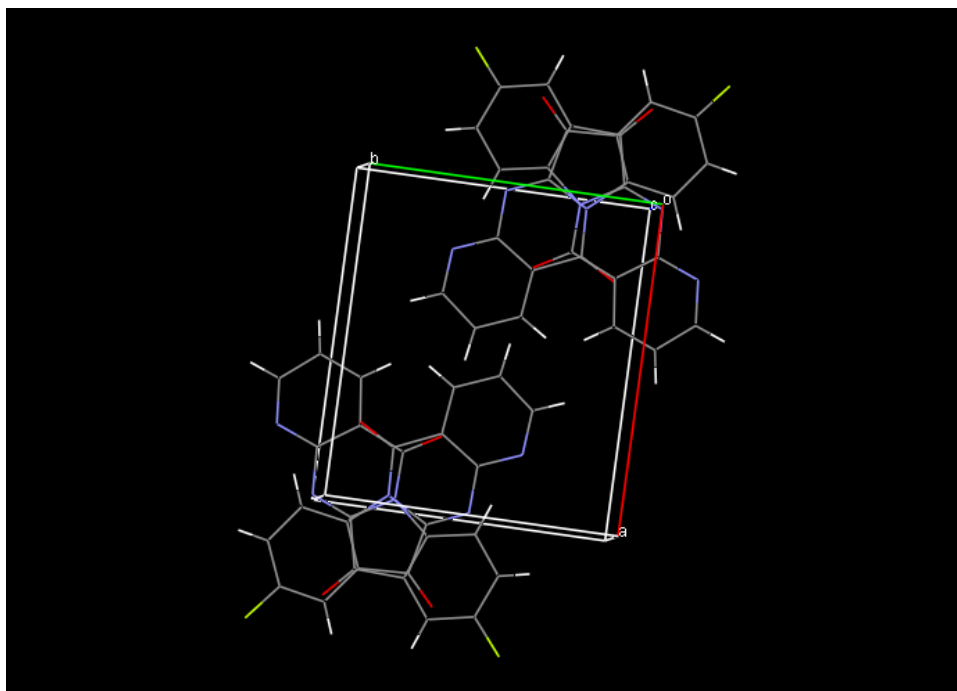
Figure 7. The crystal packing of compound **4** illustrates a crossed stacking pattern along the *c* axis.
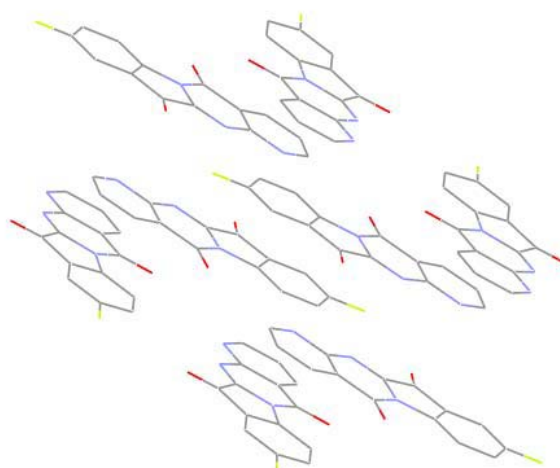

Figure 8. The molecules of compound **4** are arranged in layers tilted at a 7.64° angle relative to the (001) plane, with a 3.496(9) Å average intermolecular separation.

3.4 Inhibition of Heme Crystallization

Inhibition concentrations 50% (IC_{50}) were found for the four azaindolo[2,1–*b*]quinazoline–6,12–dione analogs. The nitro analog **1** yielded an IC_{50} of 4 µM for both hemozoin and beta hemin (Figure 9). However, the present study did not find any appreciable inhibition of heme for the other three analogs up to the 20 µM level. Nonetheless, keeping in mind the tedious nature of characterization of these adducts and the weak nature of these interactions, we are continuing our efforts to characterize these complexes and the inhibitory activity of the other analogs. However, our currently available crystallographic data on the analog **4** demonstrate the point and a weak

interaction of hemin with this class of compounds is quite probable in the line with our NMR and molecular modeling observations.
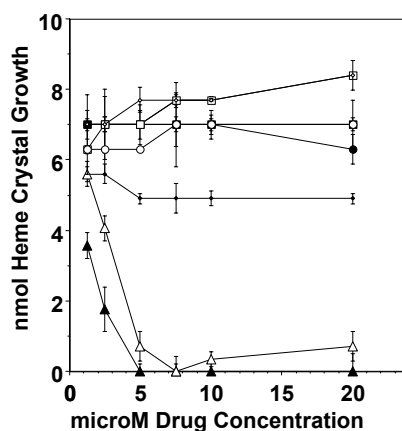
Figure 9. Heme Crystallization Inhibition. New crystal growth was measured by a checkerboard pattern of drug dilutions in 200 μl aliquots of 50 μM hemin and 1 nmol hemozoin (filled symbols solid line) or beta–hematin (open symbols dotted line). Nanomoles of new crystal growth for incorporation onto preformed crystal was determined by the equation of (2.1–O.D. 405nm) in quadruplicate samples. Error is standard deviation of four. Nitro analog **1** (triangle) inhibits at 4 μM, while **6** (square), **4** (circle) and **5** (diamond) show no inhibition.
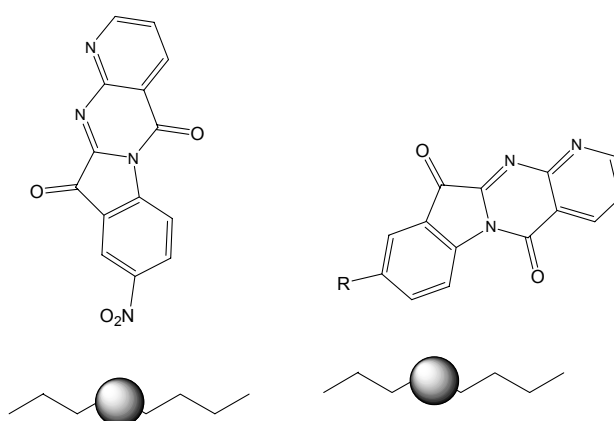
Figure 10. The binding orientation and the regions closest to the Fe^{+3} atom are different for the nitro compound **1** from that observed for the other five analogs. The gray–circle represents the Fe^{+3} atom of the hemin molecule.

4 CONCLUSIONS

In summary, our combined NMR, X–ray crystallography, and molecular modeling studies on the azaindolo[2,1–*b*]quinazoline–6,12–dione class of compounds clearly indicate the possibility of a weak *pi*–type interaction with hemin, which could be the mechanism for inhibition of polymerization of hemin and subsequent death of the malaria parasites. Experimental observation of heme crystallization of the nitro analog in this series of compounds is an indication of this possibility. However, the NMR spectra on the position of the protons, which exhibited the maximum Δδ for each analog, the 8–nitro analog **1** seems to approach hemin with a different

orientation than the other analogs tested (Figure 10). Thus, the results of this study indicate that the azaindolo[2,1–*b*]quinazoline–6,12–dione family of antimalarials may exhibit multiple paths for antimalarial activity, though inhibition of polymerization of hemin is crucial for the process. However, our data unequivocally suggests that the azaindolo[2,1–*b*]quinazoline–6,12–dione class of compounds may be therapeutically useful in the treatment of chloroquine–resistant strains of malaria. The study should aid the design and discovery of new target specific antimalarials.

Acknowledgment

5 REFERENCES

[1]   J. Wiesner, R. Ortmann, H. Jomaa, M. Schlitzer. New Antimalarial Drugs. *Angew. Chem. Int. Ed. Engl.* **2003**, *42*, 5274–5293.
[2]   P.G. Bray, S.A. Ward. A comparison of the phenomenology and genetics of multidrug resistance in cancer cells and quinoline resistance in plasmodium falciparum. *Pharmacol. Ther.* **1998**, *77*, 1–28.
[3]   A.K. Bhattacharjee, M.G. Hartell, D. Nichols, R.P. Hicks, B. Stanton, J. E. van Hamont and W. K. Milhous. Structure–activity relationship study of antimalarial indolo [2,1–b]quinazoline–6,12–diones (tryptanthrins). Three dimensional pharmacophore modeling and identification of new antimalarial candidates. *Eur. J. Med. Chem.* **2004**, *39*, 59–67.
[4]   A.F.G. Slater and A Cerami. Inhibition of chloroquine of novel haem polymerase enzyme activity in malaria trophozoites. *Nature* **1992**, *355*, 167–169.
[5]   S.R. Vippagunta, A. Dorn, H. Matile, A.K. Bhattacharjee, J.M.Karle, W.Y. Ellis, RG. Ridley and J.L. Vennerstrom. Structural Specificity of Chloroquine–Hematin binding related to inhibition of hematin polyerization and parasite growth. *J. Med. Chem.* **1999**, *42*, 4630–4639.
[6]   P.L. Oliaro and D.E. Goldberg. The plasmodium digestive vacuole: metabolic headquarters and choice drug target. *Parasitology Today* **1995**, *11*, 294–297.
[7]   J.D. Chulay. Plasmodium falciparum: Assessment of in vitro growth by [3H]hypoxanthine incorporation. *Exp. Parasitol.* **1983**, *55*, 138–146.
[8]   R.E. Desjardins, C.J. Canfield, D.E. Haynes, J.D. Chulay. Quantitative assessment of activity in vitro by a semiautomated microdilution technique. *Antimicrob. Agents Chemother.* **1979**, *16*, 710–718.
[9]   J. Bergman, J–O. Lindstrom, U. Tilstam. *Tetrahedron* **1985**, *41*, 2879–2881.
[10]   W.R. Baker, L.A. Mitscher. U.S. Patent 5 441 955 (1995)
[11]   Chemical Information System. Division of Experimental Therapeutics, Walter Reed Army Institute of Research, Silver Spring, MD 20910–7500, U.S.A.
[12]   M. J. Frisch, G.W. Trucks, H.B. Schlegel, P.M.W. Gill, B.G. Johnson, M.A. Robb, J.R. Cheeseman, T.A. Keith, G.A. Petersson, J.A. Montgomery, K. Raghavachari, M.A. Al–Laham, V.G. Zakrzewski, J.V. Ortiz, J.B. Foresman, J. Cioslowski, B.B. Stefanov, A. Nanayakkara, M. Challacombe, C.Y. Peng, P.Y. Ayala, W. Chen, M.W. Wong, J.L. Andres, E.S. Replogle, R. Gomperts, R.L. Martin, D.J. Fox, J.S. Binkley, D.J. Defrees, J. Baker, J.P. Stewart, M. Head–Gordon, C. Gonzalez and J.A. Pople, 1995, Gaussian 94 (Revision A.1), Gaussian Inc., Pittsburgh PA.
[13]   A. K. Bhattacharjee. Electrostatic potential profiles may guide cation–pi interaction in antimalarials chloroquine and mefloquine: an ab initio quantum chemical study. *J. Mol. Struct.* (*Theochem*) **2000**, *529*, 193–201.
[14]   S. Mecozzi, A.P. West, D.A. Dougherty. Cation–pi interactions in simple aromatics: electrostatic provide a predictive model. *J. Am. Chem. Soc.* **1996**, *118*, 2307–2308.
[15]   Accelrys, Inc., 9685 Scranton Road San Diego, CA 92121–3752.
[16]   C. R Chong, D. J.Sullivan. Inhibition of heme crystal growth by antimalarials and other compounds: implications for drug discovery. *Biochemical Pharmacology* **2003**, *66*, 2201–2212.

http://www.biochempress.com

[17] G. M. Sheldrick. Crystallographic Algorithms for Mini and Maxi Computers. In *Crystallographic Computing*; G.M Sheldrick, C. Krüger, R. Goddard, Eds.; Oxford University Press: Oxford, 1985; Vol. 3, pp 175–179. G.M. Sheldrick. *SHELXTL software*; University of Gőttingen: Federal Republic of Germany, 1990.

[18] G.M. Sheldrick. *SHELX–97*; University of Gőttingen: Federal Republic of Germany, 1997.

[19] S. L. Alam, B. F. Volkman, J. L. Markely, J. D. Satterlee. Detailed NMR analysis of the heme–protein interaction in component IV Glycera dibranchiata monomeric hemoglobin–CO., *J. Biomolecular NMR* **1998**, 119–133.

[20] J. Wang, Y. Li, D. Ma, H. Kalish, A. L. Balch, Solution NMR determination of the seating(s) of meso–nitro–etioheme–1 in myoglobin: Implications for steric constraints to meso position access in heme degradation by coupled oxidation. *J. Am. Chem. Soc*. **2001**, *123*, 8080–8088.

[21] S. Moreau, B. Perly, C. Chachaty, C. Deleuze et al. A nuclear magnetic resonance study of the interactions of antimalarial drugs with porphyrins. *Biochim. Biophy. Acta* **1985**, *840*, 107–116.

[22] P. N. Palma, I. Moura, J. LeGall, J. Van Beeumen, J. E. Wampler et al. Evidence for a ternary complex formed between flavodoxin and cyctochrome c3:1H NMR and molecular modeling studies. *Biochemistry* **1994**, *33*, 6394–6407.

[23] C.A. DiTusa. 8–bromoindolo(2,1–b)4–azaquinazoline–6,12–dione, CCDC 218226, private communication to the Cambridge Crystallographic Data Centre, August 26, 2003.

[24] M. Brufani, W. Fedeli, F. Mazza, A. Gerhard, W. Keller–Schierlein. The Structure of Tryptanthrin. *Experientia*. **1971**, *27*, 1249–1250.

[25] W. Fedeli, F. Mazza. Crystal Structure of Tryptanthrin(Indolo[2,1–b]quinazoline–6,12–dione). *J. Chem. Soc*. *Perkin Trans*. *II*. **1974**, 1621–1623.

Biographies

Rickey P. Hicks is a natural product chemist, received his Ph.D. in natural products chemistry from Virginia Commonwealth University under direction of Professor Albert T. Sneden in 1984. After graduation he join the staff of Nova Pharmaceutical Corporation in Baltimore Maryland. During this time his research focused on the development of novel adenosine antagonists and anti–inflammatory agents. In 1989 he joined the faculty in the Department of Chemistry at Mississippi State University, he was promoted with tenure to Associate Professor in 1994. He research at Mississippi State focused on the application of nuclear magnetic resonance spectroscopy to study the conformation induced onto linear polypeptides by micelles and lipid bilayers. He has graduated two Ph.D. and five masters students. In January 2001, he joined the staff of the Department of Medicinal Chemistry in the Division of Experimental Therapeutics at the Walter Reed Army Institute of Research as the Chief of the Nuclear Magnetic Resonance Analysis Laboratory. He has co–authored over 30 manuscripts and book chapters as well as four patents.

Charles A. DiTusa currently heads the Bio–analytical Section in the Department of Medicinal Chemistry, Division of Experimental Therapeutics, Walter Reed Army Institute of Research. He received his Ph.D. in Bio–Organic Chemistry from Duke University in 2000, under the direction of Professor Eric J. Toone. After graduation, he worked at The University of North Carolina, Chapel Hill, LC/MS Facility as a Kenan Fellow, assisting in the establishment of a campus Proteomics Core Laboratory. He then moved across campus to the Department of Environmental Science and Engineering on an NIEHS Training Grant to study protein adduct biomarkers for the quantitation of benzene exposure. He has co–authored 4 publications in peer–reviewed journals.

Apurba K. Bhattacharjee, Ph.D. is the Chief Molecular Modeler in the Department of Medicinal Chemistry at the Division of Experimental Therapeutics, Walter Reed Army Institute of Research (WRAIR), Silver Spring, Maryland, U.S.A. After obtaining Ph.D. in Physical Organic Chemistry from the North Eastern Hill University (India) in 1983, Dr. Bhattacharjee undertook postdoctoral research with Professor J.–E. Dubois at the Institut de Topologie et de Dynamique des Systemes de l'Univerite Paris 7 (France) for two and half years and returned to India to teach. He is in the current position at WRAIR since July, 1995. More recently, Dr. Bhattacharjee has collaborated on projects with Professor Jonathan Vennerstrom of College of Pharmacy, University of Nebraska and Professor Michael K. Riscoe of U.S. Veterans' Hospital, OHSU, Oregon to identify the critical molecular features of the anatimalarial, chloroquine, to reverse its resistance to the parasites. Dr. Bhattacharjee has currently undertaken a major research project to identify new antimalarial agents by targeting the fatty acid biosynthetic pathway enzymes of the parasites. He has 70 publications in major international peer reviewed journals and three patents. He is currently an advisor of the National Research Council, U.S. Academy of Sciences and mentoring postdoctoral researchers in computational chemistry studies. His extracurricular activities involve reading books and articles ranging from different philosophies of the world to religions, and international politics.

http://www.biochempress.com